

# Soft Matter

Accepted Manuscript



This is an *Accepted Manuscript*, which has been through the Royal Society of Chemistry peer review process and has been accepted for publication.

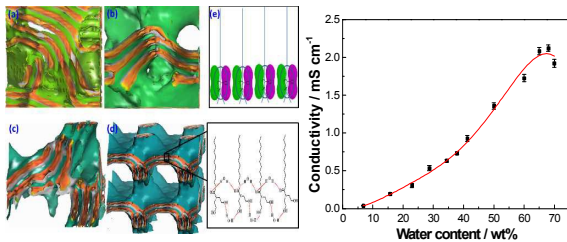
*Accepted Manuscripts* are published online shortly after acceptance, before technical editing, formatting and proof reading. Using this free service, authors can make their results available to the community, in citable form, before we publish the edited article. We will replace this *Accepted Manuscript* with the edited and formatted *Advance Article* as soon as it is available.

You can find more information about *Accepted Manuscripts* in the [Information for Authors](#).

Please note that technical editing may introduce minor changes to the text and/or graphics, which may alter content. The journal's standard [Terms & Conditions](#) and the [Ethical guidelines](#) still apply. In no event shall the Royal Society of Chemistry be held responsible for any errors or omissions in this *Accepted Manuscript* or any consequences arising from the use of any information it contains.

## Table of Contents

Ordered self-assembly of nonionic surfactant N,N-bis(2-hydroxyethyl)dodecanamide in the presence of water achieved high electric conductivity.



## ARTICLE

# High electric conductivity of liquid crystals formed by ordered self-assembly of nonionic surfactant N,N-bis(2-hydroxyethyl)dodecanamide in water

Cite this: DOI: 10.1039/x0xx00000x

Yan Zhang,<sup>a</sup> Dechun Li,<sup>\*b</sup> Yaping Li,<sup>a</sup> Sen Zhang,<sup>a</sup> Meng Wang,<sup>a</sup> Ying Li<sup>\*a</sup>

**Abstract:** This paper reported the ordered self-assembly of nonconductive small molecules achieved extra high conductivity, thereby stated a convenient approach constructing biofriendly soft material being suitable used as implantable biosensors and electro-stimulated drug delivery systems. The microstructure and the conductive mechanism were investigated in detail by combining experimental methods and molecular simulation. This research demonstrated that self-assembly of amide groups with delocalized electrons into  $\pi$ -stacked arrays exhibited high mobilities for charge carriers. The excellent biocompatibility and processability of soft materials such as liquid crystals insure the system high potential in the advance regions of biosensors and drug delivery devices.

Received 00th January 2012,  
Accepted 00th January 2012

DOI: 10.1039/x0xx00000x

www.rsc.org/

## Introduction

Molecular ordered self-assembly can induce enhanced functions.<sup>1</sup> Liquid crystals are self-assembled dynamic functional soft materials which possess both order and mobility at molecular, supramolecular and macroscopic levels.<sup>2</sup> Stacking  $\pi$ -conjugated disk-like molecules such as triphenylene, hexabenzocoronene, and phthalocyanine derivatives in liquid-crystalline columnar structures was used to prepare 1D conductive materials.<sup>3-6</sup> Some 2D conductive liquid crystalline materials also has been successful prepared by self-organization of electro-active  $\pi$ -conjugated molecules with various molecular weights.<sup>7-9</sup> Control over nanoscale ordering through self-assembly in the field of nanotechnology and biotechnology have become important because of their key roles in the development of high-performance materials.<sup>10-13</sup> Ionic liquid-crystalline (LC) materials have been shown to be good candidates for efficient ion conduction because they form well-organized nanochannels for the transportation of ions in their LC phases.<sup>14,15</sup> In this paper, we reported on an interesting discovery that liquid crystals formed by ordered self-assembly of nonionic surfactant N,N-bis(2-hydroxyethyl)dodecanamide (DDA, Scheme S1) in water achieved high electric conductivity and, for the first time, explored the conductive mechanism at a molecular level. Comparing with conductive liquid crystals self-assembled by polymers and compounds with aromatic groups, DDA liquid crystals have many advantages such as lower toxicity, easy degradation and excellent biocompatibility. In the literatures,<sup>16,17</sup> the high conductivity of organic semiconductor was correlated with the high degree of molecular ordering and a unique  $\pi$ - $\pi$  stacking of rich electronics

group. Ichikawa et al.<sup>18</sup> reported the drastic enhancement of ionic conductivity of PyZI-14/HTf<sub>2</sub>N mixture upon the addition of water which could be attributed to the change of the conduction mechanism from vehicular to hopping mechanisms.

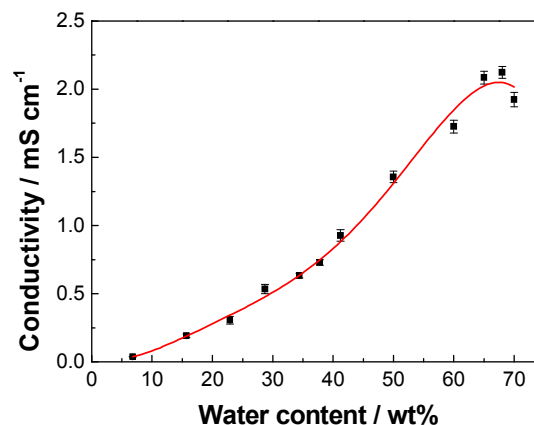


Figure 1. Conductivity of the DDA solutions as a function of water content at 40±0.01 °C.

For amphiphilic nonionic surfactant DDA, which do not meet all the above situations, the special steric effect because of the small volume of hydrophilic head groups (Scheme S1) and the coplanar conformation of amide group<sup>19</sup> with delocalized  $\pi$ -electrons might be the two important factors in exhibiting high electric conductivity in the presence of water. The proposed conductive mechanism may have significant implication in the design of novel conductive materials.

The electric conductivity of nonionic surfactant DDA is known to be ultralow. But the electric conductivity of DDA solution increased dramatically with increasing water content

(Figure 1), even reach  $2.12 \times 10^{-3} \text{ S cm}^{-1}$ , when the water content was about 68.00 wt%. After the maxima, the conductivity of the nonionic system gradually decreased with the further addition of water.

## Mechanism

The high electric conductivity achieved by simply mixing water with a nonionic surfactant is amazing, while this phenomenon cannot be explained by the conventional notions.<sup>18,20,21</sup> In order to illustrate the conductive mechanism, the micro structure of DDA-water system was investigated by deuterium NMR ( $^2\text{H-NMR}$ ), small-angle X-ray scattering (SAXS), polarizing optical microscopy (POM), freeze-fracture field emission scanning electron microscopy (FF-FESEM), and

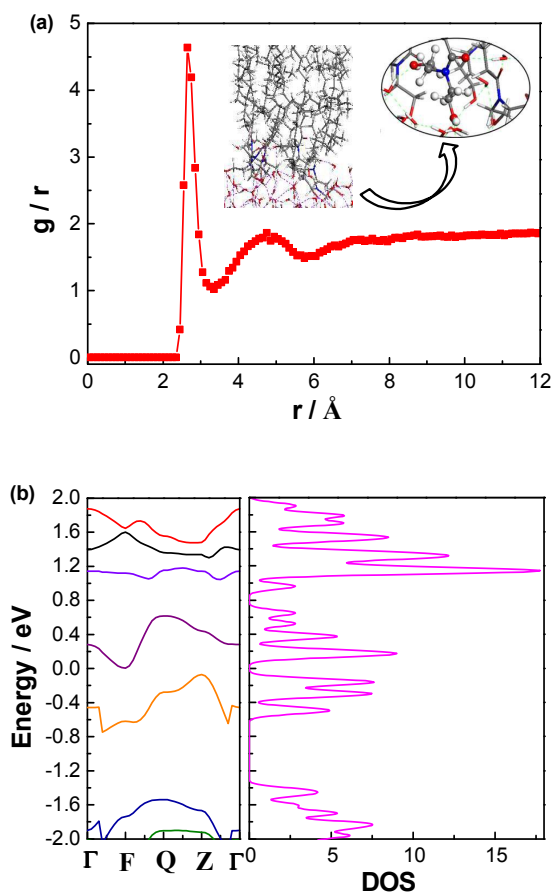


Figure 2. (a) The RDF of water molecules (the oxygen atom was assigned to be label atom) to DDA head group (the nitrogen atom was chosen to be label atom) at 40 °C. (Inset) Hydrogen-bonded networks at the DDA–water interface. The atom coloring scheme is C, gray; H, white; O, red; N, blue. (b) BS and DOS of DDA association structure calculated by first principles.

the density of states (DOS) and Band electronic structure (BS) of the DDA association structure were calculated by combining Molecular dynamics (MD) simulation and first principles calculations. By MD simulations performed through the discover module using the COMPASS force field, the microscopic details of the structural and dynamic properties of DDA assemblies were obtained. The total potential energy contains bonded terms and non-bonded terms (Eq. (1)).<sup>22</sup>

$$E_{total} = E_{bonds} + E_{angles} + E_{dihedrals} + E_{cross} + E_{non-bond} \quad (1)$$

The details of the MD simulation please see supporting information. The radial distribution function (RDF) of water molecules to DDA head group at 313K was shown in Figure 2a. The coordination number of water molecules to DDA head group was about 2. The two coordinated water molecules linked with amide and hydroxyl group of DDA through intermolecular hydrogen-bond, respectively (shown in Figure 3b), and promoted the close packing of DDA at the interface (Figure 2a inset) and the formation of the long-range ordered association

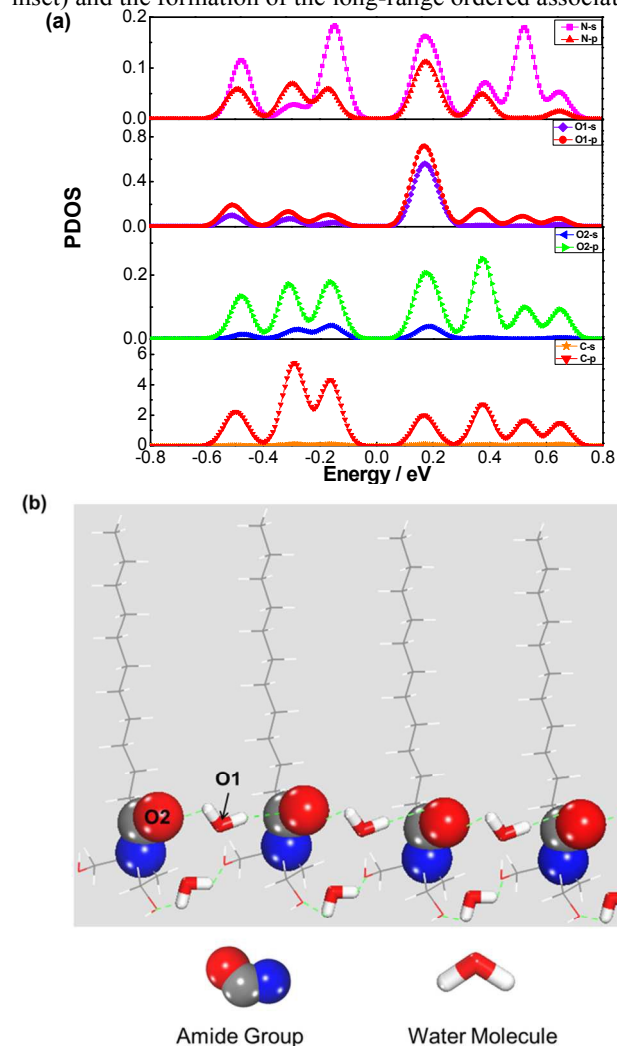


Figure 3. (a) The PDOS of N, C and O2 in amide. The PDOS of O1 from the water molecule between amide groups of DDA. The Fermi level is set to zero. (b) Schematic illustration of the proposed conductive mechanism. Blue, gray, red, and white are N, C, O, and H, respectively.

structure self-assembled by DDA molecules in water. The calculations of BS, DOS of the above DDA/water association structure were performed using Vienna ab initio simulation program (VASP, developed at the Universität Wien).<sup>23-26</sup> In Figure 2b, the Fermi level was set at 0 eV. The conduction bands located above the Fermi level and the valence bands located below the Fermi level.<sup>27,28</sup> It was found that the valence-to-conduction band gap  $E_g$  between the bottom of the conduction band and the top of the valence band in the band structure was 0.15 eV.<sup>27-30</sup> And the valence band maximum and

the conduction band minimum located at Z and F points respectively, indicating that the long-range ordered self-assembly of DDA in water constructed a kind of indirect gap semiconductor (Figure 2b).<sup>29,30</sup> For comparison, the BS of pure DDA was calculated, too. The valence-to-conduction band gap  $E_g$  of pure DDA was about 6 eV (Figure S1), which demonstrated the disordered DDA was an insulator. It could be concluded that the water molecules not only induced the ordered arrangement of DDA, but also made some key contribution to the increase of the electric conductivity of the system.

To determine charge carriers transported in the DDA-water association system, the partial density of states (PDOS) spectra were calculated by first principles, which were presented in Figure 3a. The PDOS spectra of N, O2 and C atoms of amide groups of DDA and the O1 atom of the water molecule linking with amide groups of DDA were analyzed.<sup>27,31,32</sup> As it was shown in Figure 3a, the PDOS of the C-2p orbital was far higher than that of other atomic orbitals in the range from -0.6 eV up to the Fermi level, so the C-2p orbital was crucial for the valence bands; The 2s/2p hybrid orbitals of N atom and the O2-2p orbital were also essential, too. The conduction bands mainly depend on the 2s/2p hybrid orbitals of O1 atom and 2p orbital of C atom. The results demonstrated the delocalized p- $\pi$  electrons of amide groups functioned as charge carriers transported in self-assembled networks. One of the two water molecules coordinated to the head group of DDA took part in the formation of hydrogen-bonded networks and the other linking with amide groups of DDA participated in conducting (Figure 3b). This suggested how the self-organization of DDA at a molecular level by the addition of water realized the high conductivity.

### Results and discussion

To elucidate the microstructure of DDA-water association systems, SAXS and <sup>2</sup>H-NMR techniques were used. <sup>2</sup>H-NMR spectra shown in Figure 4a exhibited that different liquid-crystalline phases were formed at various water content (30.00-68.00 wt%) at 40  $\pm$  0.01  $^{\circ}$ C. The SAXS patterns of DDA LC phase with various water content (30.00-60.00 wt%) showed intensive reflection peaks on the scattering vector ( $q$ ) axis with the reciprocal displacing ratio of 1:2 (Figure 4b), which could be indexed as (001) and (002) reflections of a lamellar LC structure. The two scattering peaks became sharper with increasing surfactant concentration, which hinted the order degree of the lamellar phase was enhanced,<sup>33</sup> and being in accordance with the <sup>2</sup>H-NMR results (Figure 4a).<sup>34-36</sup> The <sup>2</sup>H-NMR spectrum of DDA/water association system with 68.00 wt% water content at 40  $\pm$  0.01  $^{\circ}$ C contained a singlet which indicated the presence of an isotropic phase (Figure 4a). It was characterized by X-ray measurements at 40  $\pm$  0.01  $^{\circ}$ C, the relative positions of the SAXS peaks obeyed the ratio  $\sqrt{4} : \sqrt{11}$ , which could be indexed as (200), (311) reflections of a cubic structure with Fd3m symmetry (Figure 4c). The structure of the DDA liquid crystals with 68.00 wt% water content at 40  $\pm$  0.01  $^{\circ}$ C was also demonstrated by FF-FESEM micrographs in Figure 5 (a and b). Panel 5 (a) showed the bulk cubic phase structure, which could be observed more clearly at higher magnification in panel 5 (b). No polarized light diffraction texture was observed in POM of DDA/water system with 68.00 wt% water at 40  $\pm$  0.01  $^{\circ}$ C, as shown in Figure 5 (f), which agreed very well with the FF-FESEM and <sup>2</sup>H-NMR investigation.

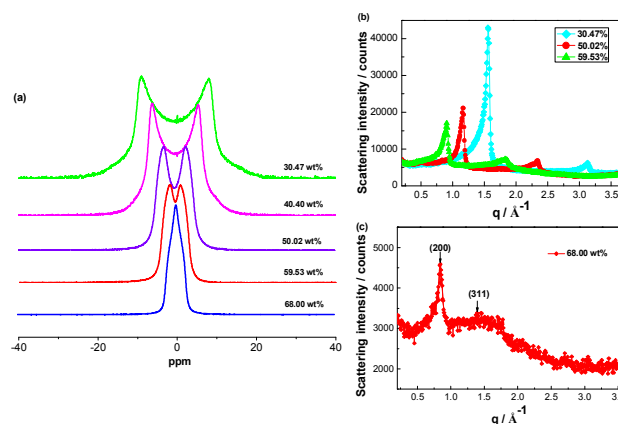


Figure 4. (a) <sup>2</sup>H-NMR spectra of DDA liquid crystals containing 30.47, 40.40, 50.02, 59.53 and 68.00 wt% water at 40  $\pm$  0.01  $^{\circ}$ C. (b) SAXS diffraction patterns of DDA liquid crystals containing 30.47, 50.02, 59.53 wt% water at 40  $\pm$  0.01  $^{\circ}$ C. (c) SAXS diffraction patterns of DDA liquid crystals containing 68.00 wt% water at 40  $\pm$  0.01  $^{\circ}$ C.

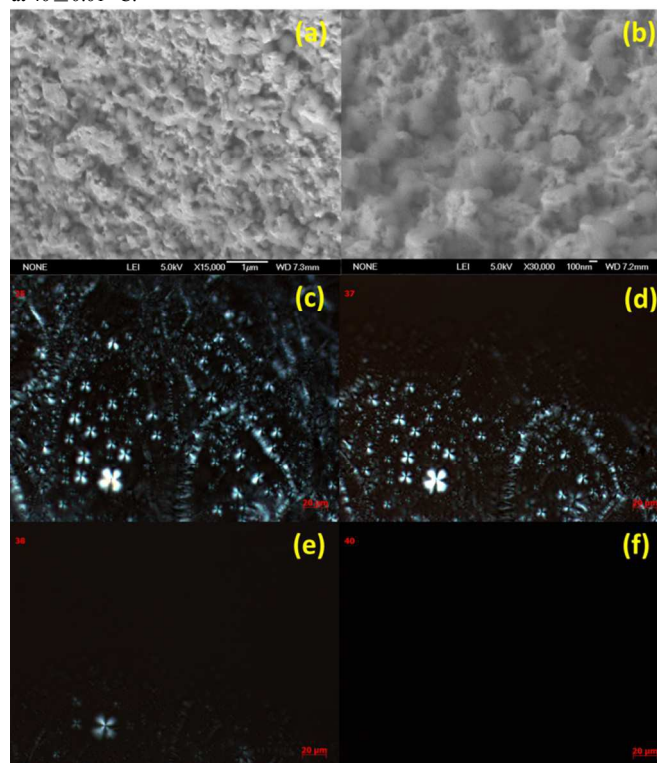


Figure 5. (a and b) FF-FESEM micrograph of Cub<sub>bi</sub> LC structure of DDA solution with 68.00 wt% water at 40  $\pm$  0.01  $^{\circ}$ C. (b) is the magnification of (a). (c-f) POM images of DDA solution containing 68.00 wt% water on heating: (c) at 25  $\pm$  0.01  $^{\circ}$ C; (d) at 37  $\pm$  0.01  $^{\circ}$ C; (e) at 38  $\pm$  0.01  $^{\circ}$ C; (f) at 40  $\pm$  0.01  $^{\circ}$ C. From (c) to (f), the phase structure transformed from the lamellar to the Cub<sub>bi</sub>.

Dissipative particle dynamics (DPD) computer simulation<sup>37</sup> was used to describe the phase structure of the DDA-water association system. The simulation details please see supporting information. The micro molecular aggregation behavior and the phase structure of the DDA/water systems containing 30.00 to 68.00 wt% water at 40  $\pm$  0.01  $^{\circ}$ C were shown in Figure 6. It was found that lamellar liquid crystals were formed in solutions with 30.00, 50.00, and 60.00 wt% water, but deformed with increasing water content (Figure 6a-c), the irregular lamellar LC structure became entangled and bicontinuous cubic (Cub<sub>bi</sub>) structure was formed in the system

with 68.00 wt% water (Figure 6d), totally echoing to the  $^2\text{H-NMR}$  and SAXS results.

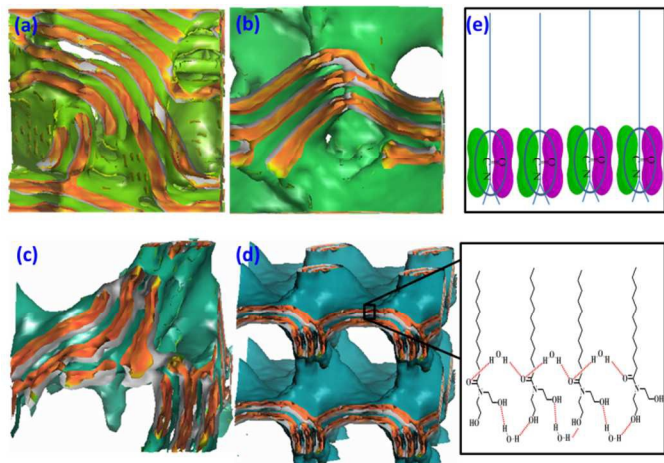


Figure 6. (a-d) Isosurface images of the simulation results of DDA/water system with 30.00, 50.00, 60.00, 68.00 wt% water at 40 °C. (e) The scheme of the distribution of the delocalized electron clouds of amide groups caused by the self-assembly of the DDA molecules.

The experimental and theoretical results bring out a reasonable explanation for the high electro-conductivity of the DDA/water association system depicted in Figure 2. SAXS,  $^2\text{H-NMR}$  and DPD results consistently showed the order degree of the lamellar phase decreased with increasing water, which meant the lamellar structure became entangled and the hydrogen-bonded networks extended from 2D to 3D. The transportation of electrons in the two-dimensional lamellar  $p-\pi$  stacking structure was less efficient than in three-dimensional  $\text{Cub}_{\text{bi}}$   $p-\pi$  stacking structure. That was why the conductivity of DDA liquid crystals with 68.00 wt% water achieved the maxima  $2122 \mu\text{S cm}^{-1}$  at  $40 \pm 0.01$  °C, when the  $\text{Cub}_{\text{bi}}$  phase having 3D successive hydrogen-bonded networks was formed. Following with the further addition of water, the structure of the DDA-water association system transformed into the lamellar again (Figure S2 and S3), so the conductivity declined. Figure 6e demonstrated the electron clouds of the  $p-\pi$  conjugated system of amide groups overlapped because the hydrophilic part of the DDA molecules arrayed closely in the long-range ordered arranged frame, which corresponded to the high transportation capacity similar to the  $\pi-\pi$  stacking of organic semiconductor.

The effect of temperature on the microstructure and conductivity of DDA liquid crystals was investigated. Figure 7a illustrated the conductivity of DDA liquid crystals containing 68.00 wt% water increased with increasing temperature, which also exhibited typical semiconductor character.<sup>38</sup> Nonlinear increases of the conductivity of DDA liquid crystals were observed in the original conductivity curve. We believed the first sudden increase of the conductivity below  $40 \pm 0.01$  °C was induced by the phase transition from lamellar to  $\text{Cub}_{\text{bi}}$  phases. At temperature above 70 °C, the deviation of the conductivity might be induced by the more closed arrangement of DDA molecules at higher temperature. The mechanism was discussed

in detail in the ESI. Differential scanning calorimetric (DSC) measurement was undertaken to study the phase transition of DDA solution with 68.00 wt% water content from -30-100 °C. On the heating process, the DSC thermogram showed two endothermic peaks at 3.1 and 34.4 °C, respectively corresponding to the melt of water molecules and a lamellar- $\text{Cub}_{\text{bi}}$  transition (Figure 7b). The phase transition from lamellar to  $\text{Cub}_{\text{bi}}$  phases was visually observed through POM Figure 5(c-f). The results agreed perfectly with the FF-FESEM (Figure 5a and b), SAXS (Figure 4c). Therefore, the delocalized electrons of  $\pi$ -stacked amide groups were transported in the long-range ordered association structure self-assembled by DDA molecules in water, and the conductivity of DDA liquid crystals linearly increased with increasing temperature in the  $\text{Cub}_{\text{bi}}$  LC phases from 40 to 70 °C.

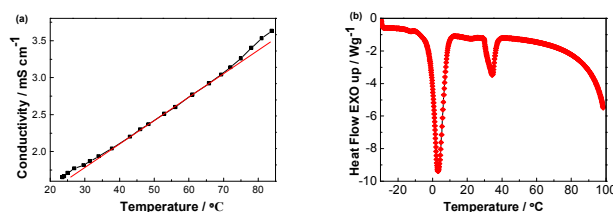


Figure 7. (a) Variation of conductivity of DDA solution with 68.00 wt% water on heating. (b) Differential scanning calorimetry thermogram of DDA solution with 68.00 wt% water.

According to the above results, the conductivity of the DDA liquid crystals can be controlled by altering water content and temperature through triggering phase transition. And the nearly linear increase of the conductivity of DDA  $\text{Cub}_{\text{bi}}$  LC phase with increasing temperature makes them promising for potential applications in thermo-sensitive conductive materials.

## Conclusions

In conclusion, a high conductive LC materials formed by self-assembly of nonionic surfactant have been found. The ordered arrangement of DDA could be switched by adjusting relative humidity and temperature, which affected the conductivity of the DDA-water association system. The first principles calculations demonstrated the long-range ordered association structure self-assembled by amphiphilic DDA molecules in water constructed an indirect gap semiconductor and the closely ordered  $p-\pi$  stacking of amide groups of DDA tightly held through intermolecular hydrogen bonds achieved high mobility of charge carriers. The coplanarity and the small volume of amide group of DDA played important roles in the high conductivity for DDA-water system. The research in the conductivity of isolated nonionic system might have significant implications for the further understanding of conductive phenomenon and provided theoretical guide to the design of new conductive materials. The high conductive DDA liquid crystals might expand their application scope in the biomedical field in the future, due to their excellent biocompatibility and processability.

## Acknowledgements

The funding from National Science Fund of China (No. 21173134, 21473103) and National Municipal Science and

Technology Project (No.2008ZX05011-002) is gratefully acknowledged. Prof. Dr. Yuxiang Bu read the PDOS section and offered helpful suggestions.

## Notes and references

<sup>a</sup> Key Laboratory of Colloid and Interface Chemistry of State Education Ministry, Shandong University, 27 Shanda Nanlu, Jinan, Shandong 250100, P. R. China.

<sup>b</sup> School of Information Science and Engineering, Shandong University, Jinan 250100, China.

Electronic Supplementary Information (ESI) available: Additional experimental information, simulation method and model of BS and DOS, and the details of MD and DPD simulations. See DOI: 10.1039/b000000x/

- 1 T. Kato, N. Mizoshita, K. Kishimoto, *Angew. Chem. Int. Ed.* 2006, **45**, 38.
- 2 (a) I. W. Hamley, *Angew. Chem.* 2003, **115**, 1730; (b) J. E. Anthony, J. S. Brooks, D. L. Eaton, S. R. Parkin, *J. Am. Chem. Soc.* 2001, **123**, 9482.
- 3 C. Liu, A. Fechtenkütter, M. D. Watson, K. MSllen, A. J. Band, *Chem. Mater.* 2003, **15**, 124.
- 4 C. D. Simpson, J. Wu, M. D. Watson, K. MSllen, *J. Mater. Chem.* 2004, **14**, 494.
- 5 A. M. van de Craats, J. M. Warman, K. MSllen, Y. Geerts, J. D. Brand, *Adv. Mater.* 1998, **10**, 36.
- 6 D. Adam, P. Schuhmacher, J. Simmerer, L. HPussling, K. Siemensmeyer, K. H. Etzbach, H. Ringsdorf, D. Haarer, *Nature* 1994, **371**, 141.
- 7 M. Funahashi, J. Hanna, *Appl. Phys. Lett.* 2000, **76**, 2574.
- 8 I. McCulloch, W. Zhang, M. Heeney, C. Bailey, M. Giles, D. Graham, M. Shkunov, D. Sparrowe, S. Tierney, *J. Mater. Chem.* 2003, **13**, 2436.
- 9 H. Kuroda, H. Goto, K. Akagi, A. Kawaguchi, *Macromolecules* 2002, **35**, 1307.
- 10 S. Choi, B.-K. Cho, *Soft Matter* 2013, **9**, 4241.
- 11 Y. Lin, Y. Qiao, P. Tang, Z. Li, J. Huang, *Soft Matter* 2011, **7**, 2762.
- 12 Y. Yan, J. Huang, *Coord. Chem. Rev.* 2010, **254**, 1072.
- 13 I. Hamley, *Soft Matter* 2011, **7**, 4122.
- 14 B. Soberats, M. Yoshio, T. Ichikawa, S. Taguchi, H. Ohno, T. Kato, *J. Am. Chem. Soc.* 2013, **135**, 15286.
- 15 (a) O. Ikkala, G. ten Brinke, *Chem. Commun.* 2004, 2131. (b) T. Ichikawa, M. Yoshio, A. Hamasaki, J. Kagimoto, H. Ohno, T. Kato, *J. Am. Chem. Soc.* 2011, **133**, 2163. (c) B.-K. Cho, *Polym. J.* 2012, **44**, 475. (d) K. Binnemans, *Chem. Rev.* 2005, **105**, 4148. (e) S. Tan, C. Wang, Y. Wu, *J. Mater. Chem. A* 2013, **1**, 1022.
- 16 X.-C. Li, H. Sirringhaus, F. Garnier, A. B. Holmes, S. C. Moratti, N. Feeder, W. Clegg, S. J. Teat, R. H. Friend, *J. Am. Chem. Soc.* 1998, **120**, 2206.
- 17 V. Coropceanu, J. Cornil, ; D. A. da Silva Filho, Y. Olivier, R. Silbey, J.-L. Brédas, *Chem. Rev.* 2007, **107**, 926.
- 18 T. Ichikawa, T. Kato, H. Ohno, *J. Am. Chem. Soc.* 2012, **134**, 11354.
- 19 A. Bennet, Q. P. Wang, H. Slebocka-Tilk, V. Somayaji, R. Brown, B. Santarsiero, *J. Am. Chem. Soc.* 1990, **112**, 6383.
- 20 B. Soberats, M. Yoshio, T. Ichikawa, S. Taguchi, H. Ohno, T. Kato, *J. Am. Chem. Soc.* 2013, **135**, 15286.
- 21 R. A. Horne, E. H. Axelrod, *J. Chem. Phys.* 1964, **40**, 1518.
- 22 T. Zhao, G. Xu, S. Yuan, Y. Chen, H. Yan, *J. Phys. Chem. B* 2010, **114**, 5025.
- 23 G. Kresse, M. Marsman, J. Furthmüller, The guide of VASP (<http://cms.mpi.univie.ac.at/vasp/vasp/vasp.html>).
- 24 J. Chanda, S. J. Bandyopadhyay, *Chem. Theory Comput.* 2005, **1**, 963.
- 25 S. S. Jang, S.-T. Lin, P. K. Maiti, M. Blanco, W. A. Goddard, P. Shuler, Y. Tang, *J. Phys. Chem. B* 2004, **108**, 12130.
- 26 J. Chanda, S. Bandyopadhyay, *J. Phys. Chem. B* 2006, **110**, 23482.
- 27 D. Li, M. Yang, S. Zhao, Y. Cai, Y. Lu, Z. Bai, Y. Feng, *Comp. Mater. Sci.* 2012, **63**, 178.
- 28 D. Li, M. Yang, Y. Cai, S. Zhao, Y. Feng, *Opt. Express* 2012, **20**, 6258.
- 29 W. R. Lambrecht, *Phys. Rev. B* 2000, **62**, 13538.
- 30 D. Li, M. Yang, S. Zhao, Y. Cai, Y. Feng, *Opt. Express* 2012, **20**, 11574.
- 31 V. L. Shaposhnikov, A. V. Krivosheeva, V. E. Borisenko, *Phys. Rev. B* 2012, **85**, 205201.
- 32 L. Yu, D. Li, S. Zhao, G. Li, K. Yang, *Materials* 2012, **5**, 2486.
- 33 Z. X. Li, J. R. Lu, R. K. Thomas, and A. Weller, *Langmuir* 2001, **17**, 5858.
- 34 M. R. de Planque, D. V. Greathouse, R. E. Koeppe, H. Schäfer, D. Marsh, J. A. Killian, *Biochem.* 1998, **37**, 9333.
- 35 A. Khan, K. Fontell, B. Lindman, *J. Colloid Interface Sci.* 1984, **101**, 193.
- 36 M. Rückert, G. Otting, *J. Am. Chem. Soc.* 2000, **122**, 7793.
- 37 R. D. Groot, P. B. Warren, *J. Chem. Phys.* 1997, **107**, 4423.
- 38 L. Pan, G. Yu, D. Zhai, H. R. Lee, W. Zhao, N. Liu, H. Wang, B. C.-K. Tee, Y. Shi, Y. Cui, *PNAS* 2012, **109**, 9287.